Bull. Mater. Sci. (2019) 42:17
https://doi.org/10.1007/s12034-018-1699-7

Microstructure and mechanical performance of (AlCrNbSiTiV)N films coated by reactive magnetron sputtering

C Y WU[1], R C HSIAO[2], C H HSU[3], T H HSIEH[3], J Y KAO[4] and C Y HSU[4,*]

[1]School of Marine Engineering, Qinzhou University, Qinzhou 535011, People's Republic of China
[2]Department of Chemical and Materials Engineering, Lunghwa University of Science and Technology, Taoyuan 33306, Taiwan
[3]Department of Materials Engineering, Tatung University, Taipei 104, Taiwan
[4]Department of Mechanical Engineering, Lunghwa University of Science and Technology, Taoyuan 33306, Taiwan
*Author for correspondence (cyhsu@mail.lhu.edu.tw)

MS received 12 January 2018; accepted 5 May 2018; published online 18 January 2019

Abstract. (AlCrNbSiTiV)N films are prepared on cermet cutter tool substrates using direct current reactive magnetron sputtering with a high-entropy alloy target. The use of a grey based Taguchi method to determine the deposition parameters of (AlCrNbSiTiV)N films has been studied by considering multiple performance characteristics. Taguchi quality design concept with an L_9 (3^4) orthogonal array, signal-to-noise ratio and analysis of variance are used to determine the performance characteristics of the deposition process. The effect of various deposition parameters of (AlCrNbSiTiV)N films on the chemical composition, the microstructure, the morphology, the mechanical performance and cutting performance of the coated cutter in dry machining is determined. The experimental results show a cutter that is coated with (AlCrNbSiTiV)N exhibits less surface roughness (for workpiece) and flank wear (for cutter), so coated cutter tools have a much longer tool life than the uncoated tools. Transmission electron microscopy patterns confirm that the (AlCrNbSiTiV)N films have a polycrystalline face-centred cubic structure. In the confirmation runs, using grey relational analysis, there are improvements of 3.7% in surface roughness, 69.6% in flank wear and 3.2% in elastic recovery. The Rockwell adhesion test categorizes the coatings as class HF1.

Keywords. High-entropy alloys; mechanical properties; cutting; grey Taguchi method.

1. Introduction

Conventional metallic alloys use one or two principal metal elements in the primary phase and minor alloying elements are added to enhance material properties [1]. Recently, there has been increasing interest in high-entropy alloys (HEAs) or multi-principal alloys, which were initially proposed by Yeh *et al* in 2004 [2]. HEAs use a novel alloy design strategy of mixing five or more constituent elements in equal or near-equal proportion to their atomic ratios, so that the concentration of each element is between 5 and 35% [3]. These HEAs have unique structures and excellent mechanical performance, with high strength and hardness values, good corrosion resistance and high temperature creep resistance [4].

Transition metal nitride films, such as ZrN, ZrWN, TiN and TiAlN, are the subject of much study because they exhibit high-hardness values and good-wear resistance and adhere well to the substrates [5]. Alloying appropriate elements into binary nitride film coatings (ternary or quaternary systems) modifies the properties of the coating. Therefore, HEAs exhibit appropriate features and properties for nitride films [6]. Using transmission electron microscopy (TEM) and X-ray diffraction (XRD) analysis, various HEA nitride films that contain mixtures of nitride and non-nitride elements exhibit both amorphous and nanocrystalline structures [7]. The HEA nitride coating exhibits a single face-centred cubic (FCC) structure with good mechanical properties [8].

The Taguchi method increases experimental efficiency because it combines experimental design theory and the quality loss function. It is used in products that feature reduced cost and improved quality [9]. The mixed orthogonal table for the Taguchi quality design procedure identifies important control factors and a statistical analysis of signal-to-noise (S/N) ratio is followed by an analysis of variance (ANOVA) [10]. Chen *et al* [11] used a grey based Taguchi method to determine the processing parameters for a CrWN thin film coating by considering multiple levels of performance. Das *et al* [12] used a grey based Taguchi analysis to optimize the parameters for an electroless Ni–B coating using multiple response outputs, in order to minimize the friction and wear characteristics. Several techniques are used to grow nitride films. Sputtering is a suitable technique for the deposition of nitride films because it is low cost and offers good uniformity over large areas [13].

This study deposits HEA (AlCrNbSiTiV)N films on cermet cutter tools (T1000A) using direct current (DC) reactive magnetron sputtering. Four factors, each of which has three levels, are used to determine the effect of control factors (DC power,

Table 1. Factor setting levels for the deposition of (AlCrNbSiTiV)N using reactive sputtering.

Substrates	Cermet cutter tool (T1000A) and SUS304
Target	$Al_{17.0}Cr_{16.3}Nb_{17.5}Si_{17.1}Ti_{16.3}V_{15.8}$ (purity 99.99%)
Gas	Ar and N_2 (purity 99.95%)
Total gas flow	20 sccm
Base pressure	7.5×10^{-6} Torr
Substrate-to-target distance	85 mm
Substrate rotate speed	10 rpm
Working pressure	1.0×10^{-3} Torr
Deposition time	20 min

(AlCrNbSiTiV)N thin film coated

Symbol	Control factor	Level 1	Level 2	Level 3
A	DC power (W)	120	150	180
B	Substrate temperature (°C)	200	300	400
C	$N_2/(N_2 + Ar)$ (%)	10	20	30
D	Substrate bias (−V)	80	100	120

Table 2. The dry turning parameters.

Workpiece material	SUS304 stainless steel, 40 mm diameter
Cutting tool	With and without (AlCrNbSiTiV)N coated
Cutting fluid	Dry cutting
Cutting length	75 mm
Spindle speed	1250 rpm
Feed rate	1.2 mm per rev
Depth of cut	1.5 mm

substrate temperature, $N_2/(N_2 + Ar)$ flow rate and substrate bias) on the deposition of (AlCrNbSiTiV)N films. An L_9 (3^4) orthogonal array is used. Table 1 lists the settings for the factors and levels for the deposition of (AlCrNbSiTiV)N films. Grey relational analysis [14] is used to study multiple performance characteristics for the Taguchi method, in order to optimize the coating process for (AlCrNbSiTiV)N films. Dry cutting is a common manufacturing process that has low overhead costs and reduces the impact on the environment [15]. This study dry turns SUS304 stainless steel using a cermet cutter with these HEA (AlCrNbSiTiV)N thin film coatings. The structure and surface morphology of the nanostructure of the coatings are determined using scanning electron microscopy (SEM) and TEM systems. The micro-hardness, elastic modulus, elastic recovery and film's adhesion are also determined.

2. Experimental

The HEA sputtering targets used equiatomic amounts of Al, Cr, Nb, Si, Ti and V elements and were produced by vacuum electric arc melting at least four times. The target composition was determined using energy dispersive spectrometry. The composition is $Al_{17.0}Cr_{16.3}Nb_{17.5}Si_{17.1}Ti_{16.3}V_{15.8}$. The (AlCrNbSiTiV)N films were deposited on cermet cutter tool substrates using DC magnetron sputtering with a base pressure of 7.5×10^{-6} Torr. The AlCrNbSiTiV alloy targets of 99.99% purity and a mixture of high purity 99.95% Ar plasma and N_2 reactive gas were used. A constant distance was maintained between the substrate and the target (85 mm) and a constant rotational speed was maintained for the substrate (10 rpm). Pre-sputtering was performed for 5 min, in order to clean and equilibrate the target surface prior to deposition.

The typical chemical composition and mechanical properties for SUS304 stainless steel are given in [16]. In this study, coated cermet cutter tools were mounted on a low-cost conventional lathe (CH-400, KINWA Machine Tool Co. Ltd., Taiwan) and used to cut cylindrical SUS304 stainless steel workpieces (table 2). To ensure the reproducibility of results, all tests were performed twice and average values are presented.

A profilometer (Suftest-402 Mitutoyo) was used for R_a measurements. The thickness of the films was measured using a surface profilometer (α-step, ET-4000A). The morphology of the coatings was determined using a field emission scanning electron microscope (SEM, JEOL JSM-6500F). Microstructural examinations used an analytical TEM system (Philips Tecnai F20 G2 FEI-TEM). The chemical composition of the films was determined using an electron probe X-ray microanalyzer (JXA-8200, EPMA), with a spatial resolution of more than 1 μm. The films' structural properties were determined using XRD (Rigaku-2000 X-ray Generator), using CuKα radiation (40 kV, 30 mA and $\lambda = 0.1541$ nm) and grazing incidence optics, in order to increase the sensitivity of the near-surface region. The micro-hardness, the elastic modulus and the elastic recovery values for the (AlCrNbSiTiV)N thin film coatings were determined using a nanoindenter (ASMEC UNAT).

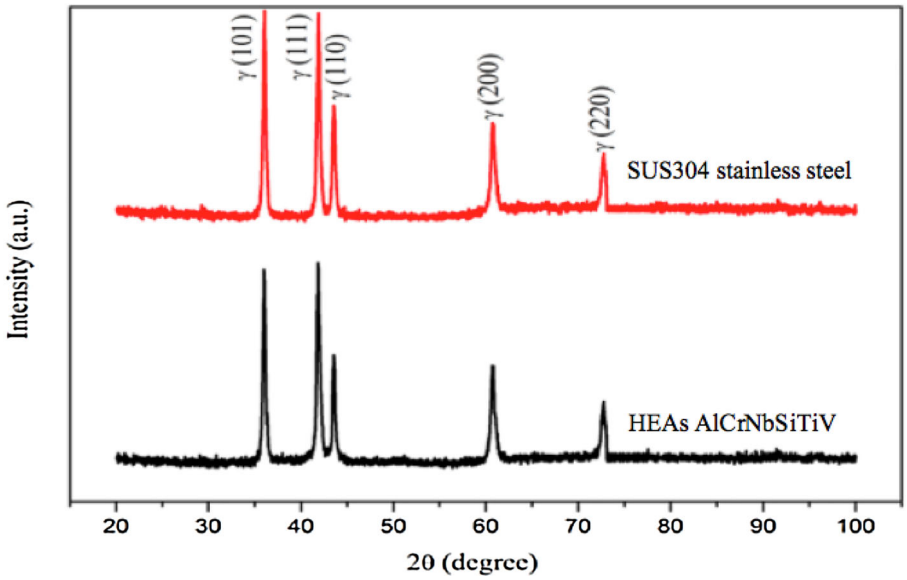

Figure 1. XRD patterns for the AlCrNbSiTiV metallic films coated onto SUS304 stainless steel.

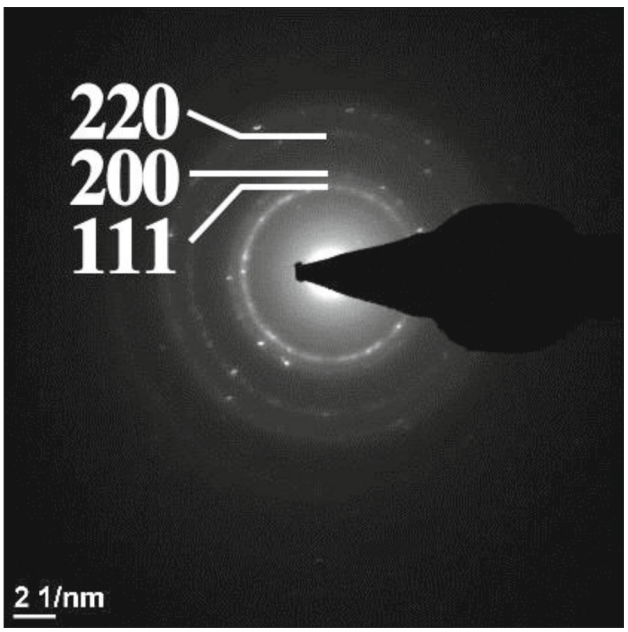

Figure 2. TEM micrographs of the (AlCrNbSiTiV)N films coated with the SAD patterns.

3. Results and discussion

3.1 *Properties of HEA (AlCrNbSiTiV)N films*

AlCrNbSiTiV metallic and nitride films were deposited using DC reactive magnetron sputtering. The structure of the films was determined using grazing incidence XRD, with an angle of incidence of 2°, in order to increase the sensitivity of the near-surface structure. Figure 1 shows the XRD

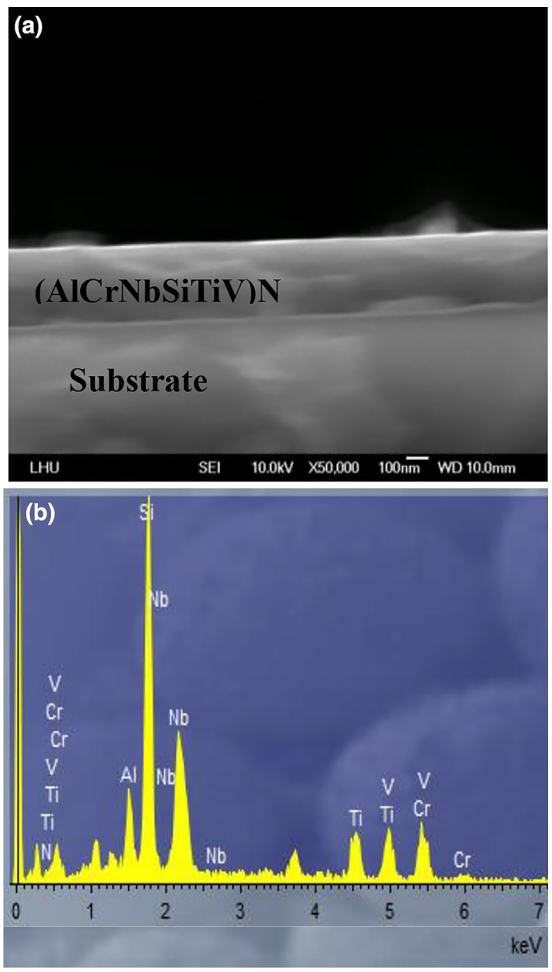

Figure 3. (AlCrNbSiTiV)N film coatings: (**a**) cross-sectional SEM image and (**b**) EPMA spectrum.

Table 3. The thickness and EPMA analysis composition of HEA (AlCrNbSiTiV)N films, for numbers 1–9 of the L_9 orthogonal array.

No.	Factors				Elements (at%)							Film thickness (average, nm)
	A	B	C	D	Al	Cr	Nb	Si	Ti	V	N	
1	1	1	1	1	10.43	11.83	8.62	11.17	9.78	10.53	37.64	252
2	1	2	2	2	8.44	8.83	6.41	12.60	7.45	7.88	48.39	175
3	1	3	3	3	7.45	7.40	5.35	9.14	6.47	6.69	57.50	160
4	2	1	2	3	7.84	8.12	5.98	7.19	7.01	7.34	56.52	204
5	2	2	3	1	8.90	9.79	6.82	7.64	8.03	8.60	50.22	210
6	2	3	1	2	9.48	12.35	8.38	13.76	9.82	10.86	35.35	238
7	3	1	3	2	7.20	10.43	5.80	10.50	7.39	8.62	50.06	255
8	3	2	1	3	7.09	8.77	6.26	9.30	8.41	8.82	51.35	295
9	3	3	2	1	7.48	8.97	6.60	13.97	7.84	7.57	47.57	286

Note: A, DC power (W); B, substrate temperature (°C); C, $N_2/(N_2 + Ar)$ flow rate (%); D, substrate bias (−V).

Table 4. The experimental results and S/N ratios for the surface roughness and flank wear using a cermet tool coated with (AlCrNbSiTiV)N films for dry turning (experiments were run twice).

No.	Factors				Surface roughness (R_a, μm)			Flank wear (μm)		
	A	B	C	D	T1	T2	S/N (dB) lower is better	T1	T2	S/N (dB) lower is better
1	1	1	1	1	1.10	1.06	− 0.67	34.4	36.0	− 30.93
2	1	2	2	2	0.91	0.76	1.53	25.9	29.6	− 28.88
3	1	3	3	3	1.16	0.95	− 0.51	20.4	15.9	− 25.24
4	2	1	2	3	1.04	1.19	− 0.97	5.40	5.80	− 14.97
5	2	2	3	1	0.89	0.78	1.55	9.00	10.0	− 19.57
6	2	3	1	2	0.94	1.12	− 0.29	10.8	12.2	− 21.23
7	3	1	3	2	1.12	0.88	− 0.06	14.9	17.1	− 24.10
8	3	2	1	3	0.86	0.77	1.76	14.5	15.6	− 23.56
9	3	3	2	1	1.04	1.12	− 0.67	14.3	16.8	− 23.86
Uncoated tool					1.94	2.08		39.6	40.8	

Table 5. The ANOVA results for the surface roughness and flank wear, corresponding to table 4.

Factors	S/N ratio (dB)			Degree of freedom	Sum of squares	Variance	Contribution (P, %)
	Level 1	Level 2	Level 3				
Surface roughness							
A	0.12	0.10	0.34	2	0.11	0.06	1.13
B	− 0.57	1.61	− 0.49	2	9.19	4.59	94.55
C	0.27	− 0.04	0.33	2	0.23	0.11	2.37
D	0.07	0.39	0.10	2	0.19	0.10	1.95
Total				8	9.72		100
Flank wear							
A	− 28.35	− 18.59	− 23.84	2	143.31	71.66	79.13
B	− 23.34	− 24.00	− 23.45	2	0.77	0.38	0.43
C	− 25.24	− 22.57	− 24.74	2	12.42	6.21	6.86
D	− 24.79	− 24.74	− 21.26	2	24.60	12.30	13.58
Total				8	181.10		100

Table 6. The grey relational grade and its order in the optimization process.

No.	Factors A	B	C	D	Grey relational grade	Order
1	1	1	1	1	0.3474	9
2	1	2	2	2	0.6414	4
3	1	3	3	3	0.4629	8
4	2	1	2	3	0.6667	3
5	2	2	3	1	0.8368	1
6	2	3	1	2	0.5630	5
7	3	1	3	2	0.5175	6
8	3	2	1	3	0.8051	2
9	3	3	2	1	0.4797	7

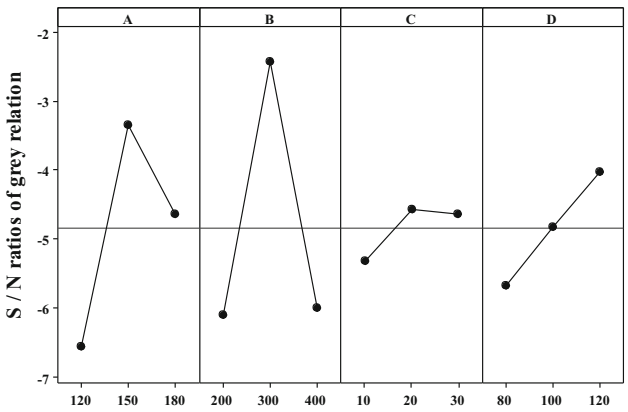

Figure 4. The S/N response graph for the grey relational grade.

patterns of the HEA AlCrNbSiTiV metallic films that are coated onto stainless steel substrates. The pattern of a stainless steels substrate is also shown for comparison. The AlCrNbSiTiV metallic films exhibit nearly the same pattern as the substrate, with only the XRD reflections of the stainless steel being seen in both diffraction patterns. This demonstrates that the deposited metallic film has an amorphous structure. The effect of a high-mixing entropy and very differently sized atoms increases the complexity of the deposited HEA metallic films and favours an amorphous structure [17]. HEAs exhibit ideal features and properties for nitride films [18]. Figure 2 shows the TEM micrographs, with the selected area diffraction (SAD) pattern of the (AlCrNbSiTiV)N film coatings, confirm that the nitride films have a polycrystalline FCC structure, which correspond to the (111), (200) and (220) planes. This result is in agreement with the results of Liang and Hsueh *et al* [19,20]. The stresses relax away from the interface between HEA nitride films and the substrate so the lattice order begins to form nano-grains and crystal columns that the FCC structure begins to develop. Lin *et al* [21] reported that HEA metallic films exhibit an amorphous structure and FCC phases appear when the amount of nitrogen flux that is used in the sputtering process is increased.

Figure 3a and b shows cross-sectional SEM images of (AlCrNbSiTiV)N films and the corresponding EPMA spectrum. The SEM micrographs show that the films are very dense and homogeneous and that they adhere perfectly to the substrate. EPMA analysis was carried out several times to measure the chemical composition of the films.

The thickness and EPMA analysis composition of HEA (AlCrNbSiTiV)N films, for numbers 1–9 of the L_9 orthogonal array are shown in table 3. It is seen that the average film thickness ranges from 160 to 295 nm. The relative atomic concentration of each element in the (AlCrNbSiTiV)N films is comparable with that in the HEA target. This is also in agreement with the results of Huang *et al* [22]. The (AlCrNbSiTiV)N films form a solid solution of different nitrides, such as the stoichiometric (metal)N type [23].

Dry machining is a non-polluting cutting process that reduces environmental impact. This study uses dry cutting SUS304 stainless steel using cutter tools that are uncoated or coated with (AlCrNbSiTiV)N hard-film coatings. Table 4 shows that after turning with tools that are coated with (AlCrNbSiTiV)N (orthogonal arrays from no. 1 to 9), the surface roughness (for workpiece) ranges from 0.82 to 1.12 μm, and flank wear (for cutter) ranges from 5.60 to 35.20 μm. If uncoated tools are used, the respective values for surface roughness and flank wear are 2.01 and 40.20 μm. The experimental results demonstrate that using a tool that is coated with (AlCrNbSiTiV)N produces a significant decrease in the surface roughness and flank wear. Coated tools have a much longer life than the uncoated tools. Table 5 lists the results for the ANOVA for surface roughness and flank wear (corresponding to table 4). The substrate temperature ($P = 94.55\%$) has the greatest effect on the surface roughness and the DC power is the most significant factor for flank wear, with $P = 79.13\%$ contribution.

Table 7. Results for the confirmation experiment for the multiple performance characteristics for the orthogonal array and the optimal predicted deposition parameters.

	Orthogonal array $A_2B_2C_3D_1$	Grey theory prediction design $A_2B_2C_2D_3$	Improvement rate (%)
(AlCrNbSiTiV)N coated tool in dry turning SUS304			
Roughness (μm)	0.84	0.81	3.7
Flank wear (μm)	9.50	5.60	69.6

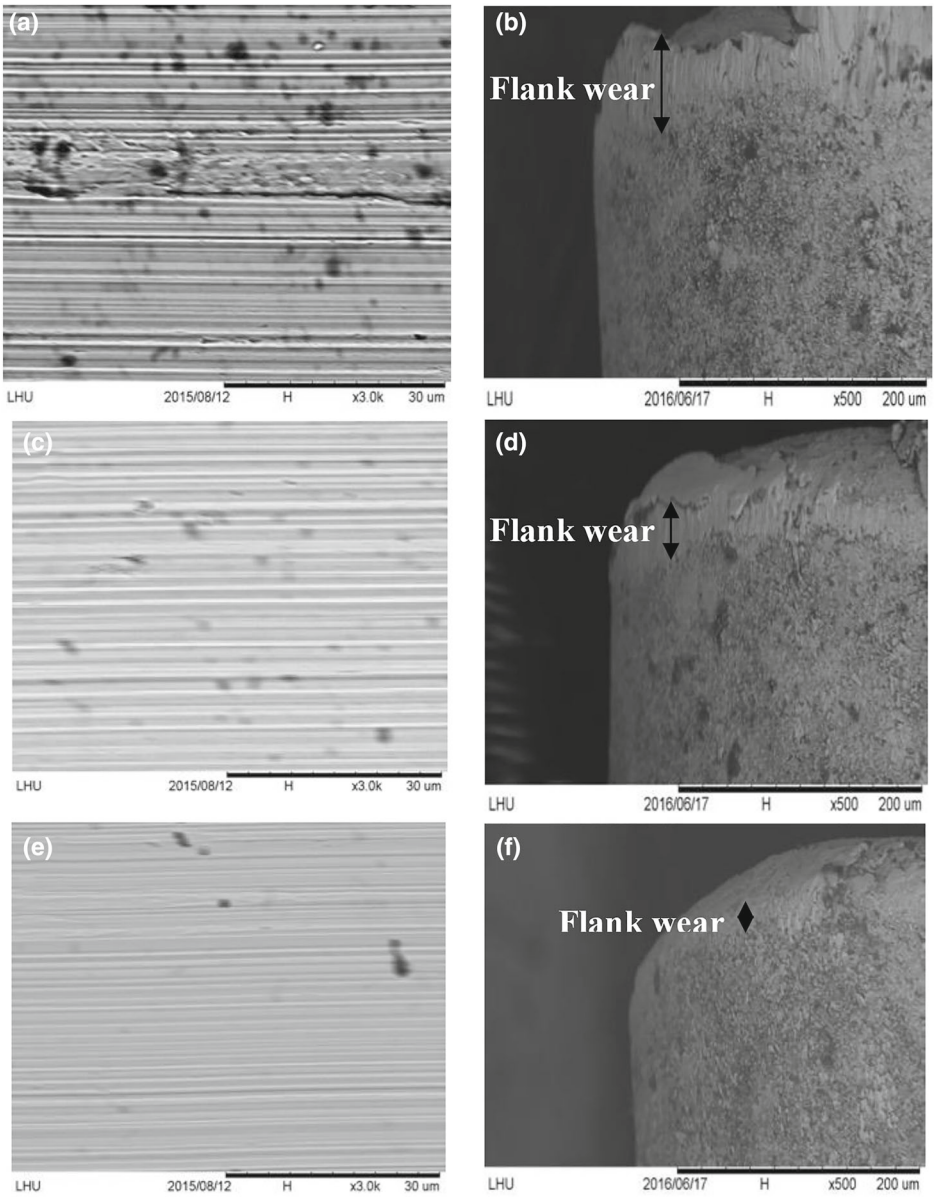

Figure 5. A comparison of the cutting surface of the machined workpiece (**a**, **c** and **e**) and the flank wear for the cermet cutting tool (**b**, **d** and **f**), with or without a (AlCrNbSiTiV)N coating: (**a**, **b**) uncoated cermet tool, (**c**, **d**) coated with (AlCrNbSiTiV)N using the $A_2B_2C_3D_1$ orthogonal array deposition parameters and (**e**, **f**) coated with (AlCrNbSiTiV)N using the $A_2B_2C_2D_3$ grey theory design deposition parameters.

Table 8. The ANOVA results for the grey relational grade for tools that are coated with (AlCrNbSiTiV)N.

Factor	Degree of freedom	Sum of square	Variance	Contribution (P, %)
A	2	15.78	7.89	33.05
B	2	26.69	13.35	**55.89**
C	2	1.08	0.54	2.26
D	2	4.20	2.10	8.80
Total	8	47.75		100

Table 9. The effect of the substrate temperature on surface roughness and flank wear (cermet tool T1000A) for tools that are coated with (AlCrNbSiTiV)N and used in dry turning SUS304.

Constant deposition parameters	150 W DC power, 20% $N_2/(N_2 + Ar)$ flow rate, − 120 V substrate bias		
Changing substrate temperature (°C)	250	300	350
(AlCrNbSiTiV)N coated tool in dry turning SUS304			
Roughness (μm)	0.92	0.81	0.91
Flank wear (μm)	10.81	5.60	9.97

3.2 *Optimal parameters for the deposition of HEA (AlCrNbSiTiV)N films*

This study optimizes the deposition parameters for cutting tools that are coated with (AlCrNbSiTiV)N using grey relational analysis, which is used extensively in various industries. The grey relational coefficient is given by [24]:

$$r(x_0(k), x_i(k)) = \frac{\min\limits_i \min\limits_k \left|x_0(k) - x_i(k)\right| + \zeta \max\limits_i \max\limits_k \left|x_0(k) - x_i(k)\right|}{\left|x_0(k) - x_i(k)\right| + \zeta \max\limits_i \max\limits_k \left|x_0(k) - x_i(k)\right|} \quad (1)$$

where $x_i(k)$ is the normalized value of the kth performance characteristic in the ith experiment and ζ is a distinguishing coefficient: $\zeta \in \lfloor 0, 1 \rfloor$. The value of ζ can be adjusted according to the actual system requirements. The parameters for the (AlCrNbSiTiV)N coating are equally weighted in this study, so ζ is 0.5.

The grey relational grade is a weighted sum of the grey relational coefficient. It is defined as:

$$r(x_0, x_i) = \frac{1}{n} \sum_{k=1}^{n} r(r_0(k), x_i(k)) \quad (2)$$

where n is the number of performance characteristics [24].

The grey relational grade for each experiment in the L_9 orthogonal array is shown in table 6. The calculation uses equations (1 and 2). A higher grey relational grade corresponds to an experimental result that is closer to the ideal normalized value. Since ($A_2B_2C_3D_1$, no. 5) has the highest grey relational grade, these are the best performance characteristics from the nine experiments. Figure 4 shows that the optimum conditions for multiple performance characteristics for the (AlCrNbSiTiV)N film coating are given by the combination, $A_2B_2C_2D_3$, which corresponds to a DC power of 150 W, a substrate temperature of 300°C, a $N_2/(N_2 + Ar)$ flow rate of 20% and a substrate bias of −120 V. Table 7 lists the results for the confirmation experiment for the multiple performance characteristics for the orthogonal array and the optimal predicted deposition parameters. A comparison of the grey theory prediction design with the orthogonal array parameters shows that the surface roughness of the machined workpiece is decreased from 0.84 to 0.81 μm and the flank wear for the cutting tool is decreased from 9.50 to 5.60 μm. These figures represent respective improvements of 3.7 and 69.6%. Figure 5 compares the machined workpieces (a, c

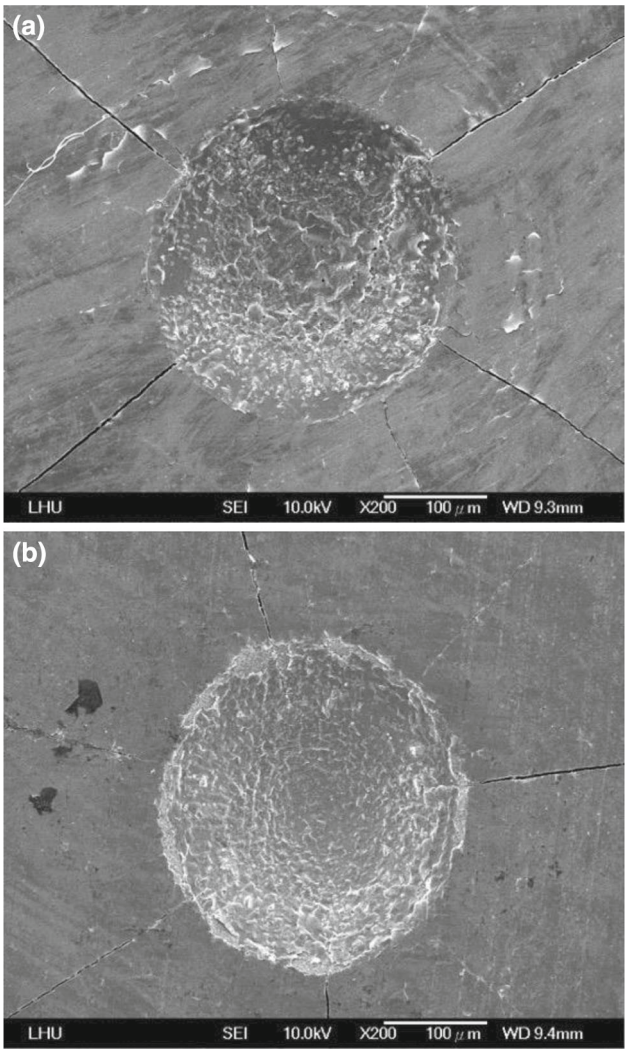

Figure 6. The optical microscope morphology for the Rockwell C indentation test for a (AlCrNbSiTiV)N coating: (**a**) the orthogonal array deposition parameters ($A_2B_2C_3D_1$) and (**b**) the grey theory prediction design ($A_2B_2C_2D_3$). Note: Adhesion classes are identified using VDI-3198.

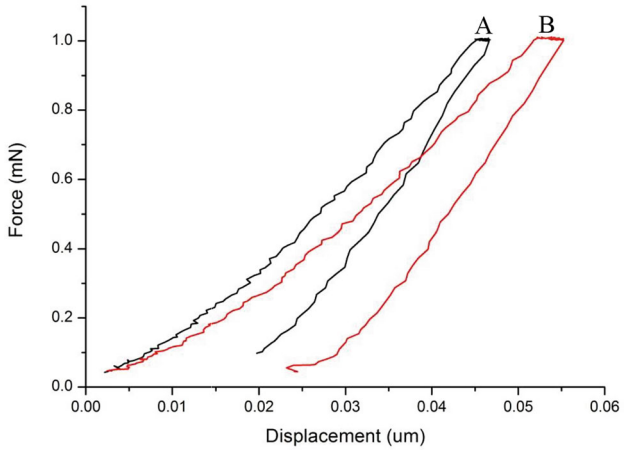

Mechanical properties of (AlCrNbSiTiV)N films

	orthogonal array B	grey theory predicted design A	Improvement rate (%)
Hardness, H (GPa)	8 (0.26 Stdev.)	10.31 (0.58 Stdev.)	28.9
Elastic modulus, E (GPa)	113.8 (1.77 Stdev.)	148.4 (1.37 Stdev.)	30.4
Elastic recovery (%R_e)	62 (1.34 Stdev.)	64 (1.73 Stdev.)	3.2
H/E ratio	0.07	0.07	

Figure 7. The nanoindentation load–displacement curves for (AlCrNbSiTiV)N films. The peak force is loaded at 1 mN. B shows the result for the orthogonal array parameters and A shows the result for the grey relational analysis prediction. Note: We adopt the 'one standard deviation' as the error bar in our analysis.

and e) and the flank wear (b, d and f) for cutters with or without a (AlCrNbSiTiV)N coating. The cutting performance is improved when coated tools are used. It is significant that for the coated tool using the $A_2B_2C_2D_3$ grey theory design deposition parameters, the machined surface of the workpiece shows fewer surface defects (figure 5e) and the cutter exhibits reduced flank wear (figure 5f). Table 8 lists the ANOVA results for the grey relational grade for the tools that are coated with (AlCrNbSiTiV)N. It is seen that the substrate temperature is the most significant factor for both the surface roughness and flank wear. To determine the effect of substrate temperature, temperatures of 250, 300 and 350°C were used and other variables from the grey theory prediction were fixed. Table 9 shows the effect of the substrate temperature on surface roughness and flank wear (cermet tool T1000A) for tools that are coated with (AlCrNbSiTiV)N and used for dry turning SUS304. This study finds that a substrate temperature of 300°C produces the lowest values for surface roughness and flank wear.

Rockwell C indentation tests were conducted using a total load of 150 kg to determine the adhesion of the coatings. Gerth and Wiklund [25] reported six classes (HF1–HF6) for indentations that qualitatively measured the adhesion of thin films to their substrates. Figure 6 shows the morphology of the Rockwell C indentation for the (AlCrNbSiTiV)N film coatings. In figure 6a for the coating using the orthogonal array deposition parameters, class HF2 shows a higher density of cracks in the coating around the indentation. In figure 6b, for the coating using the grey theory prediction design, class HF1 is characterized by fewer cracks.

The nanomechanical properties of the films are presented in terms of the depth to which the indenter penetrates at maximum load (h_{max}), the depth of the residual indent (h_r) and the elastic recovery (R_e) [26]. Figure 7 shows typical nanoindentation load–displacement curves for (AlCrNbSiTiV)N films. The peak force is loaded at 1 mN. For coatings that are deposited using the orthogonal array deposition parameters, $h_{max} = 56.5$ nm, $h_r = 20.5$ nm and $R_e = 64\%$ and for coatings that are deposited using the grey relational analysis predicted deposition parameters, $h_{max} = 46.5$ nm, $h_r = 17.5$ nm and $R_e = 62\%$. The values for the hardness (H), the elastic modulus (E), H/E and the elastic recovery for the (AlCrNbSiTiV)N films are given. The optimum (AlCrNbSiTiV)N coating has the highest values for hardness, elastic modulus and H/E.

4. Conclusions

This study deposits HEA (AlCrNbSiTiV)N films on cermet tool substrates using DC reactive magnetron sputtering.

The cutting tools are then used for dry turning. An L_9 (3^4) orthogonal array and the grey Taguchi method are used to determine the performance characteristics of the coating process. The AlCrNbSiTiV metallic films exhibit an amorphous structure and TEM patterns confirm that the nitride films have a FCC structure. A comparison of the grey theory prediction design and the parameters for the orthogonal array for the tool that is coated with (AlCrNbSiTiV)N shows that the surface roughness of the machined workpiece decreases from 0.84 to 0.81 μm and the flank wear for the cutting tool decreases from 9.50 to 5.60 μm. These represent a respective improvement of 3.7 and 69.6%. The Rockwell C indentation test for the (AlCrNbSiTiV)N coating that uses the parameters for the grey theory prediction characterizes it as class HF1. It has fewer cracks. Overall, the results show the grey Taguchi method simplifies the process of optimizing complicated multiple performance characteristics.

Acknowledgements

The authors gratefully acknowledge the support of the School of Marine Engineering, Qinzhou University, Qinzhou 535011, China, 2017 KYQD211, and Lunghwa University of Science and Technology, Taiwan.

References

[1] Li D Y and Zhang Y 2016 *Intermetallics* **70** 24
[2] Yeh J W, Chen S K, Lin S J, Gan J Y, Chin T S, Shun T T *et al* 2004 *Adv. Eng. Mater.* **6** 299
[3] Sathiaraj G D, Bhattacharjee P P, Tsai C W and Yeh J W 2016 *Intermetallics* **69** 1
[4] Cai Z, Jin G, Cui X, Li Y, Fan Y and Song J 2016 *Vacuum* **124** 5
[5] Subramanian B, Prabakaran K and Jayachandran M 2012 *Bull. Mater. Sci.* **35** 505
[6] Cheng K H, Lai C H, Lin S J and Yeh J W 2011 *Thin Solid Films* **519** 3185
[7] Lai C H, Cheng K H, Lin S J and Yeh J W 2008 *Surf. Coat. Technol.* **202** 3732
[8] Chen T K, Wong M S, Shun T T and Yeh J W 2005 *Surf. Coat. Technol.* **200** 1361
[9] Jayabal S and Natarajan U 2011 *Bull. Mater. Sci.* **34** 1563
[10] Gupta A, Singh H and Walia R S 2016 *Bull. Mater. Sci.* **39** 1223
[11] Chen G C, Hu C C, Wang C H, Lu T W and Hsu C Y 2013 *Int. J. Refract. Met. Hard Mater.* **37** 82
[12] Das S K and Sahoo P 2011 *Mater. Des.* **32** 2228
[13] Addepalli S and Suda U 2016 *Bull. Mater. Sci.* **39** 789
[14] Hu C C, Lu T W, Chou C Y, Wang J T, Huang H H and Hsu C Y 2014 *Bull. Mater. Sci.* **37** 1275
[15] Basavakumar K G, Mukund P G and Chakraborty M 2007 *Bull. Mater. Sci.* **30** 427
[16] Barshilia H C and Rajam K S 2007 *Bull. Mater. Sci.* **30** 607
[17] Huang P K and Yeh J W 2009 *Surf. Coat. Technol.* **203** 1891
[18] Shen W J, Tsai M H, Chang Y S and Yeh J W 2012 *Thin Solid Films* **520** 6183
[19] Liang S C, Chang Z C, Tsai D C, Lin Y C, Sung H S, Deng M J *et al* 2011 *Appl. Surf. Sci.* **257** 7709
[20] Hsueh H T, Shen W J, Tsai M H and Yeh J W 2012 *Surf. Coat. Technol.* **206** 4106
[21] Lin C H, Duh J G and Yeh J W 2007 *Surf. Coat. Technol.* **201** 6304
[22] Huang P K and Yeh J W 2009 *Thin Solid Films* **518** 180
[23] Lai C H, Lin S J, Yeh J W and Chang S Y 2006 *Surf. Coat. Technol.* **201** 3275
[24] Deng J L 1989 *J. Grey Syst.* **1** 1
[25] Gerth J and Wiklund U 2008 *Wear* **264** 885
[26] Barshilia H C and Rajam K S 2004 *Bull. Mater. Sci.* **27** 35